

# EMPIRICAL CONSTRAINTS ON THE GR ELECTRIC FIELD ASSOCIATED WITH PSR J0437-4715

C. VENTER<sup>1</sup> AND O.C. DE JAGER<sup>2</sup>

*Unit for Space Physics, North-West University, Potchefstroom Campus,  
Private Bag X6001, Potchefstroom, 2520, South Africa*

## ABSTRACT

We simulate the magnetosphere of the nearby millisecond pulsar PSR J0437-4715, which is expected to have an unscreened electric potential due to the lack of magnetic pair production. We incorporate General Relativistic (GR) effects and study curvature radiation (CR) by primary electrons, but neglect inverse Compton (IC) scattering of thermal X-ray photons by these electrons. We find that the CR spectrum cuts off at energies below  $\sim 17$  GeV, well below the threshold of the H.E.S.S. telescope ( $\lesssim 100$  GeV), while other models predict a much higher cutoff of  $\gtrsim 100$  GeV. GR theory also predicts a relatively narrow pulse ( $\beta^o \sim 0.2$  phase width) centered on the magnetic axis. EGRET observations above 100 MeV significantly constrain the application of the Muslimov & Harding (1997) model for  $\gamma$ -ray production as a result of GR frame dragging, and ultimately its polar cap (PC) current and accelerating potential. Whereas the standard prediction of this pulsar's  $\gamma$ -ray luminosity due to GR frame dragging is  $\sim 10\%$  of the spindown power, a non-detection by forthcoming H.E.S.S. observations will constrain it to  $\lesssim 0.3\%$ , enforcing an even more severe revision of the accelerating electric field and PC current.

*Subject headings:* stars: neutron — pulsars: individual(PSR J0437-4715)

## 1. INTRODUCTION

Several authors have included General Relativistic (GR) frame dragging in models of pulsar magnetospheric structure and associated radiation and transport processes, recognising it to be a first order effect (see e.g. Muslimov & Harding 1997 (MH97); Dyks, Rudak, & Bulik 2001).

---

<sup>1</sup>fskcv@puk.ac.za

<sup>2</sup>fskocdj@puk.ac.za

Usov (1983) was the first to suggest that the low magnetic field strengths of millisecond pulsars (MSPs) allow  $\gamma$ -rays up to at least 100 GeV to escape pair production. Most MSPs have (largely) unscreened electric fields due to the low optical depths of primary curvature  $\gamma$ -rays for pair production in such low-B pulsar magnetospheres (Harding, Muslimov, & Zhang 2002, HMZ02). Radiation reaction limited curvature  $\gamma$ -rays up to about 100 GeV from MSPs have been predicted (HMZ02; Bulik, Rudak, & Dyks 2000, BRD00), making nearby MSPs such as PSR J0437-4715 (Johnston et al. 1993) attractive targets for ground-based  $\gamma$ -ray groups (BRD00; Venter 2004). The unscreened case offers a test for fundamental GR electrodynamical derivations of the polar cap (PC) current and potential, without having to invoke additional modifications such as pair formation fronts (Harding & Muslimov 1998, HM98) with associated slot gaps (Muslimov & Harding 2003) to explain most observations of canonical (high-B) pulsars.

The use of an unscreened GR electric field (see section 2) for PSR J0437-4715 (implied by its relatively low spindown power - HMZ02) was justified *a posteriori* (see section 3). Several important parameters, most notably its mass and distance (Van Straten et al. 2001), are accurately known, making PSR J0437-4715 one of the closest pulsars to earth and probably much brighter and easier observable than other MSPs. Also, observations show that the radio and X-ray beams virtually coincide (Zavlin et al. 2002), implying that the observer sweeps through the approximate center of the PC (Manchester & Johnston 1995; Gil & Krawczyk 1997).

In this paper, we investigate the effect of GR constraints on MSP spectral cutoffs, pulse profiles, integral flux and conversion efficiency of spindown power to  $\gamma$ -ray luminosity by simulating (using a finite element approach) radiative and transport processes which occur in a pulsar magnetosphere.

## 2. THE UNSCREENED ELECTRIC FIELD AND RADIATIVE LOSSES

We use the GR-corrected expressions for a static dipolar magnetic field (e.g. Muslimov & Tsyganskii 1992 (MT92); MH97) and curvature radius  $\rho_c$  (e.g. HM98) of an oblique pulsar with magnetic moment  $\mu = B_0 R^3 / 2$  inclined at an angle  $\chi$  relative to the spin axis. The value of the surface magnetic field (at the pole),  $B_0$ , was solved for using (MH97)

$$\dot{E}_{\text{rot}} \equiv I \Omega \dot{\Omega} \approx \frac{B_0^2 \Omega^4 R^6}{6c^3 f^2(1)}, \quad (1)$$

with  $\dot{E}_{\text{rot}}$  the spindown power,  $\Omega$  the angular speed,  $\dot{\Omega}$  the time-derivative thereof,  $I$  the moment of inertia,  $R$  the stellar radius,  $c$  the speed of light in vacuum and  $f(\eta)$  defined by

eq. (25) of MT92.

The effect of GR frame dragging on the charge density, electric potential and hence the magnitude of  $E_{||}$  (the electric field component parallel to the local magnetic field lines) was carefully modelled for the unscreened case, since the optical depth for magnetic pair production above the PC is insignificantly small (see section 3). The ‘near’ and ‘distant’ cases for  $E_{||}$  (when  $\eta \simeq 1$  and  $\eta \gg 1$ , with  $\eta = r/R$ ), coincide at different points for different pulsar parameters. We use the same framework as Harding, Muslimov and Tsygan (MT92; MH97; HM98), with all the symbols corresponding to their formalism. For the ‘near’ case,

$$E_{||}^{\text{near}} = -\frac{\Phi_0}{R} \{ 12\kappa\Theta_0^2 s_1 \cos\chi + 6s_2\Theta_0^3 H(1)\delta(1) \sin\chi \cos\phi \}, \quad (2)$$

with the vacuum potential  $\Phi_0 \equiv B_0\Omega R^2/c$ , compactness parameter  $\kappa = \epsilon I/MR^2$ ,  $\epsilon = 2GM/Rc^2$ , pulsar mass  $M$ , polar angle of last closed magnetic field line  $\Theta(\eta) = [(\Omega R\eta/cf(\eta))]^{1/2}$  and  $\Theta_0 \equiv \Theta(1)$  (HM98). Furthermore, in eq. (2),

$$s_1 = \sum_{i=1}^{\infty} \frac{J_0(k_i \xi)}{k_i^3 J_1(k_i)} [1 - e^{-\gamma_i(1)(\eta-1)}] \quad (3)$$

$$s_2 = \sum_{i=1}^{\infty} \frac{J_1(\tilde{k}_i \xi)}{\tilde{k}_i^3 J_2(\tilde{k}_i)} [1 - e^{-\tilde{\gamma}_i(1)(\eta-1)}], \quad (4)$$

with  $k_i$  and  $\tilde{k}_i$  the positive roots of the Bessel functions  $J_0$  and  $J_1$ ,  $\xi \equiv \theta/\Theta(\eta)$  the normalised polar angle,  $\phi$  the magnetic azimuthal angle, and  $H(1)\delta(1) \approx 1$ . (For  $\gamma_i$  and  $\tilde{\gamma}_i$ , see eq. [22] in HM98 and definitions following eq. [43] in MT92). Note that  $E_{||}^{\text{near}}(\eta = 1) = 0$  as required by the boundary conditions and that  $E_{||}$  scales linearly with radial distance  $\eta$  close to the stellar surface (derived from a Taylor expansion of eq. [3] and eq. [4] at  $\eta \sim 1$ ). For the ‘far’ case ( $\eta > R_{PC}/R$ ), we use (HM98)

$$E_{||}^{\text{far}} \simeq -\frac{\Phi_0}{R} (1 - \xi^2) \Theta_0^2 \left\{ \frac{3}{2} \frac{\kappa}{\eta^4} \cos\chi + \frac{3}{8} \Theta(\eta) H(\eta) \delta(\eta) \xi \sin\chi \cos\phi \right\}, \quad (5)$$

and for the corotating charge density  $\rho_e$ , we use eq. (32) in MT92.

The change in the energy of a primary electron is given (when only the dominating curvature radiation (CR) component is considered, neglecting inverse Compton (IC) scattering and synchrotron radiation) by

$$\frac{dE}{dt} = e\beta_r c E_{||} - \frac{2}{3} \left( \frac{e^2 c}{\rho_c^2} \right) \gamma^4, \quad (6)$$

with  $e$  the electron charge,  $\beta_r = v_e/c \sim 1$  the normalised electron speed and  $\gamma$  the Lorentz factor. The photon energy  $\epsilon_\gamma$  is set equal to the characteristic CR energy  $\epsilon_c \equiv 1.5(\lambda_c/\rho_c)\gamma^3$  (in units of  $m_e c^2$  - Luo, Shibata, & Melrose (2000)), with  $\lambda_c = \hbar/m_e c \approx 3.86 \times 10^{-11}$  cm the Compton wavelength.

### 3. PAIR PRODUCTION, SPECTRA AND CUTOFFS

According to HMZ02, the CR death line is at  $\dot{E}_{\text{rot}} \lesssim 10^{35} \text{ erg s}^{-1}$ . Evaluating  $\dot{E}_{\text{rot}} = -4\pi I \dot{P}/P^3 \sim 4 \times 10^{33} \text{ erg s}^{-1}$  (using the corrected intrinsic period derivative  $\dot{P}$  - Van Straten et al. (2001)) suggests that no pair production will take place. Detailed modelling yields negligible optical depths, confirming this scenario. This is indeed fortunate because of the limited number of free parameters in this case. However, a low intensity of IC scattered UV photons/soft X-rays into the TeV range may contribute to a weak pair production component.

For the parameter ranges  $R_6 \equiv R/10^6 \text{ cm} = 1.3 - 1.7$  (e.g. Kargaltsev, Pavlov, & Romani 2004),  $I_{45} \equiv I/10^{45} \text{ g.cm}^2 = 1 - 3$  (e.g. HMZ02), and  $(\chi, \zeta) = (35^\circ, 40^\circ)$  (Manchester & Johnston 1995),  $(\chi, \zeta) = (20^\circ, 25^\circ)$  (e.g. Pavlov & Zavlin 1997) and  $(\chi, \zeta) = (20^\circ, 16^\circ)$  (Gil & Krawczyk 1997), with  $\zeta$  the observer angle, the maximum CR cutoff energy is obtained by using  $R_6 = 1.3$ ,  $I_{45} = 3$  and  $\chi = 20^\circ$ . We used  $M = 1.58M_\odot$  derived from Shapiro delays (Van Straten et al. 2001). This corresponds to  $\kappa \sim 0.2$  and surface magnetic field strength  $B_8 \equiv B_0/10^8 \text{ G} \sim 7.2$  (see eq. [1]). The relative altitude for maximum CR energy is obtained as  $\eta \sim 1.47$  corresponding to a normalized field line colatitude of  $\xi \sim 0.1$  and  $\rho_c \sim 10^8 \text{ cm}$ , while the magnetic azimuth  $\phi = 0$  results in a maximum GR potential. The analytical expression for the maximum  $\gamma$ -ray energy is obtained by combining eq. (5), (6), and the expression for  $\epsilon_\gamma$ , giving

$$\epsilon_{\gamma, \text{max}} = \left(\frac{3}{2}\right)^{7/4} \lambda_c \left(\frac{\beta_r E_{||}}{e}\right)_{\text{max}}^{3/4} \rho_c^{1/2} \lesssim 17 \text{ GeV.} \quad (7)$$

One of the most interesting predictions from MH97 is that the primary electron luminosity is given by (assuming  $\chi \sim 0$ ):

$$L_{\text{prim}, \text{max}}^{\chi=0} \sim \frac{3}{4} \kappa (1 - \kappa) \dot{E}_{\text{rot}}. \quad (8)$$

It is important to note that the electric potential and charge density were derived assuming that electrons leave the PC with a speed equal to  $c$ . Even if the stellar injection speed  $\beta_{RC} \ll c$ , it can be shown that the electrons will become relativistic very close to the neutron star surface, making maximum electron energies virtually independent of the injection speed (also: A.K. Harding 2004, personal communication). The bolometric particle luminosity of a single PC will therefore be given by (MH97)

$$L_{\text{prim}} = \alpha c \int |\rho_e| \Phi dS, \quad (9)$$

with  $\Phi$  the electric potential and  $dS$  the element of spherical surface cut by the last open field lines at radial distance  $r$ . Integrating over  $\xi$  and  $\phi$ , and letting  $\eta \rightarrow \infty$ , we obtain

(Venter 2004)

$$L_{\text{prim,max}} = L_{\text{prim,max}}^{|\chi=0} \left\{ \cos^2 \chi + \left( \frac{3\Theta_0 H(1) [\pi/2 - \Theta_0 H(1)]}{16\kappa(1-\kappa)} \right) \sin^2 \chi \right\}, \quad (10)$$

providing we adopt a value of  $\Theta(\eta) = \pi/2$  for distances  $\eta > c/\Omega R$ . This result reduces back to eq. (8) when  $\chi$  is set equal to zero. We calculated the maximum efficiency of conversion of pulsar spindown power into particle luminosity  $L_{\text{prim,max}}$  for  $\chi = 20^\circ$  and  $\chi = 35^\circ$ , and obtained  $\sim 2 - 11\%$  for PSR J0437-4715, for each PC (depending on  $R$  and  $I$ , using  $M = 1.58M_\odot$ ). We also obtained the bolometric photon luminosity  $L_\gamma$  using a finite element (particle tracing) approach and integrating numerically over all photon energies and field lines from the surface to the light cylinder:

$$L_\gamma = \int_0^{\Theta_0} \int_0^{2\pi} \left( \dot{N}(\phi_R, \theta_R) \int_{r=R}^{r=c/\Omega} P_\gamma(\phi, \theta, r) dt \right) d\phi d\theta. \quad (11)$$

Here  $P_\gamma$  is the CR photon power integrated over frequency and  $\dot{N} = \rho_e c dS/e$  the number of particles ejected per second from a PC surface patch  $dS$  at  $r = R$  centered at  $(\phi_R, \theta_R)$ . Since we cannot start with  $\beta_R = 1$  (i.e. infinite Lorentz factor), we assumed values close to 1 and found convergent photon luminosities of 2–9% of the spindown power (depending on  $R, I, \chi$  and  $\zeta$ ), i.e.  $L_\gamma/L_{\text{prim,max}} \sim 1$ . This means that almost all particle luminosity is converted to photon luminosity as expected for strong radiation reaction. Radiation reaction, combined with further (weak) acceleration towards the light cylinder, result in a total residual electron power of  $\sim 1 - 2.5\%$  of the spindown power at the light cylinder.

It should be noted that the fundamental unscreened expression for  $E_{||}$  (eq. [5]) changes sign along  $\sim 40\%$  of the magnetic field lines originating at the PC. This field reversal is most dominant when  $\phi \sim \pi$ , whereas no field reversals occur for  $\phi \sim 0$ . Trapping of electrons may ensue at magnetic field lines along which the electric field reverses. We expect the system to reach a steady state as a result of the redistribution of charges along these field lines. These lines may become equipotential lines, or a reduced current may develop, resulting in the suppression of particle acceleration along them. This justifies our neglect of these field lines when calculating the pulse profiles, bolometric photon luminosity and integral flux.

Figure 1 shows the pulse profiles for different observer angles  $\zeta$ , for  $\chi = 35^\circ$ . Maximum observed photon flux is obtained for  $\zeta \sim \chi$  and for large values of  $\cos \phi$  (as in eq. [5]). The ‘dip’ in light curves with  $\zeta \geq \chi$  near phase  $\phi_L/2\pi \sim 0.5$  (where  $\phi \sim \pi$ ) might be due to the sign reversal of the electric field, because the magnetic field lines where this sign reversal occur, were ignored as noted above.

The differential photon power  $dL_\gamma(\phi_L, \zeta, E)/d\phi_L d\zeta dE$  per phase bin  $d\phi_L$ , per observer angle bin  $d\zeta$ , per energy bin  $dE$ , is obtained by inserting the product of the ratios of indicator functions  $I(\phi_L, \phi_L + d\phi_L)$ ,  $I(\zeta, \zeta + d\zeta)$  and  $I(E, E + dE)$  and their respective bin widths  $d\phi_L$ ,  $d\zeta$  and  $dE$  in the integrand of eq. (11). This allows us to compare the expected integral photon flux with EGRET upper limits above 100 MeV and 1 GeV (Fierro et al. 1995), as well as with forthcoming H.E.S.S. observations of this pulsar (Venter 2004). Note that the imaging threshold energy of H.E.S.S. is  $\sim 100$  GeV (Hofmann 2001), although a non-imaging “pulsar trigger” for timing studies down to  $\gtrsim 50$  GeV can be employed for pulsar studies with H.E.S.S. (de Jager et al. 2001).

The phase-averaged photon flux (as would be seen on a DC skymap) for a single PC may be calculated by

$$\bar{F}_\gamma^o(>E) = \frac{\beta^o}{d^2 \bar{\Delta\Omega}^o} \int_E^\infty \int_\zeta^{\zeta+d\zeta} \int_0^{2\pi} \frac{1}{E'} \left[ \frac{dL(\phi'_L, \zeta', E')}{d\phi'_L d\zeta' dE'} \right] d\phi'_L d\zeta' dE', \quad (12)$$

with distance  $d = 139$  pc,  $\beta^o = \Delta\phi_L/2\pi$ ,  $\Delta\phi_L$  the pulse width in radians,  $\bar{\Delta\Omega}^o(>E) = \sin\zeta d\zeta \Delta\phi_L$  the beaming solid angle, and  $d\zeta$  taken arbitrarily small. Only one PC is expected to be seen, given the relative orientations of the magnetic axis and observer line-of-sight to the spin axis. The superscript ‘o’ will be used to indicate quantities applicable to an observer with  $\zeta \in (\zeta, \zeta + d\zeta)$ .

The energy spectrum  $dL/dE$  due to CR is quite hard, resulting in a constant time-averaged integrated photon flux  $\bar{F}_\gamma^o(>E)$ , seen by the observer, as shown in figure 2 (e.g. curves (a) and (b)). The 100 MeV and 1 GeV EGRET flux upper limits from Fierro et al. (1995) are indicated by the squares on figure 2, which clearly constrain the flux band defined by (a) and (b). If we define an *a priori* phase interval of  $\beta^o \sim 0.2$ , centered on the radio pulse, and recalculate the EGRET flux upper limits from the factor five ( $= 1/\beta^o$ ) reduced skymap background, we should get the even more constraining upper limits given by the diamonds in figure 2. We therefore have to revise the predicted fluxes for PSR J0437-4715 and we do so based on the following scaling argument: If we assume that the particle and hence  $\gamma$ -ray luminosity only scales with the spindown power and neutron star compactness, as in eq. (8) and eq. (10), i.e. the product of the current and voltage for such a pair-starved pulsar is a constant as predicted by eq. (8), we may scale the set of curves (a) through (c) (according to this condition of a constant photon luminosity  $L_\gamma^o$ ) in terms of the limiting voltage and hence the cutoff energy to give  $\bar{F}_{\gamma,1}^o(>E_1) \times E_{\text{cutoff},1} \sim \bar{F}_{\gamma,2}^o(>E_2) \times E_{\text{cutoff},2}$  (for constant  $\beta^o$  and  $\bar{\Delta\Omega}^o$ , and energies  $E_1 < E_2$ ;  $E_{\text{cutoff},1} < E_{\text{cutoff},2}$ ). In particular, when curve (c) is scaled according to  $E_{\text{cutoff},2} = \lambda E_{\text{cutoff},1}$ , implying  $\bar{F}_{\gamma,2}^o(>E_2) \sim \bar{F}_{\gamma,1}^o(>E_1)/\lambda$ , with  $\lambda = 400$ , curve (d) is obtained, which no longer violates the revised EGRET upper limit at 1 GeV, but the cutoff energy then shifts up to  $\sim 1$  TeV. Furthermore, if curve (d) is now translated so

that the energy cutoff also falls below the H.E.S.S. sensitivity curves, curve (e) is obtained, which would be consistent with both EGRET and H.E.S.S. (if the latter instrument does not detect this pulsar). Also shown is the flux band calculated for PSR J0437-4715 by BRD00. Again, for a power-law photon spectrum with exponential cutoff, it can be shown that  $\bar{F}_\gamma^o(>E_1)E_{\text{cutoff}} \sim \beta^o L_\gamma^o / d^2 \Delta\Omega^o$  (assuming  $E_1 \ll E_{\text{cutoff}}$ , and  $\bar{F}_\gamma^o(>E)$  having a flat slope due to CR). In order to constrain PSR J0437-4715’s bolometric photon luminosity by forthcoming H.E.S.S. observations, we postulate that  $L_\gamma = \alpha L_\gamma^o$ , where  $\alpha = \alpha(\chi, \zeta) \gg 1$  is a geometrical factor correcting from the incremental luminosity corresponding to the observer’s line-of-sight, to the total  $\gamma$ -ray luminosity of the pulsar. It then follows that  $L_\gamma \sim x \bar{F}_\gamma^o(>E_1)E_{\text{cutoff}}$ , with  $x(\chi, \zeta) = \alpha d^2 2\pi \sin \zeta d\zeta$ , which was found to be more or less constant for the same  $\chi$  and  $\zeta$ . A non-detection by H.E.S.S., as implied by curve (e), leads to a  $\gamma$ -ray luminosity of  $\lesssim 0.003 \dot{E}_{\text{rot}}$ . This value should be compared with the prediction of  $L_\gamma \sim 3 \times 10^{-5} \dot{E}_{\text{rot}}$  given by Rudak & Dyks (1999) for a canonical pulsar with  $P = 1$  ms and  $B_0 = 10^9$  G and with  $L_\gamma \sim 0.04 \dot{E}_{\text{rot}}$  predicted for pair-starved pulsars with off-beam geometry (using  $P \approx 5.76$  ms and  $\dot{E}_{\text{rot}} \sim 4 \times 10^{33}$  erg.s $^{-1}$  - Muslimov & Harding (2004)).

#### 4. CONCLUSIONS

CR cutoff energies for MSPs such as PSR J0437-4715 were predicted to be in the range 50 – 100 GeV by HMZ02 and BRD00, making proposals for ground-based telescopes with imaging thresholds near 100 GeV (e.g. H.E.S.S. (Hofmann 2001) and CANGAROO (Yoshida, Yoshikoshi, & Yuki 2002)) attractive. From the present GR theory, one would conclude that these telescopes may not be able to see the spectral tail corresponding to the intense primary CR component, since the hard primary CR spectrum does not extend to energies above  $\sim 20$  GeV, as verified by both analytical and numerical (finite element) approaches. An IC component resulting from TeV electrons scattering the UV/soft X-rays from the surface of PSR J0437-4715 may however still be detectable, although this prediction by BRD00 should also be re-evaluated within a GR electrodynamical framework. However, it is quite obvious that the predicted time-averaged observer flux violates the EGRET upper limit at 100 MeV, implying a revision of the existing theory. Forthcoming H.E.S.S. and future GLAST observations will help to constrain the  $\gamma$ -ray luminosity, and therefore the accelerating electric field.

The authors would like to acknowledge useful discussions with A.K. Harding, B. Rudak and A. Konopelko. This publication is based upon work supported by the South African National Research Foundation under Grant number 2053475.

## REFERENCES

Bulik, T., Rudak, B., & Dyks, J. 2000, MNRAS, 317, 97 (BRD00), arXiv:astro-ph/9912274

de Jager, O.C., Konopelko, A., Raubenheimer, B.C., & Visser, B. 2001, in High Energy Gamma-Ray Astronomy, AIP Proc. Vol. 558, ed. F.A. Aharonian & H.J. Völk (New York: AIP), 613, arXiv:astro-ph/0010179

Dyks, J., Rudak, B., & Bulik, T. 2001, Proc. of the 4th INTEGRAL Workshop, ed. A. Gimenez, V. Reglero & C. Winkler (ESA SP-459, Noordwijk), p. 191, arXiv:astro-ph/0010301

Fierro, J.M., et al. 1995, ApJ, 447, 807

Gil, J., & Krawczyk, A. 1997, MNRAS, 285, 561

Harding, A.K., & Muslimov, A.G. 1998, ApJ, 508, 328 (HM98), arXiv:astro-ph/9805132

Harding, A.K., Muslimov, A.G., & Zhang, B. 2002, ApJ, 576, 366 (HMZ02), arXiv:astro-ph/0205077

Hinton, J.A. 2004, New Astron. Rev., 48, 331, arXiv:astro-ph/0403052

Hofmann, W. 2001, in Proc. of the 27th ICRC (Hamburg: Copernicus Gesellschaft), OG2.5, 2785

Johnston, S., et al. 1993, Nature, 361, 613

Kargaltsev, O., Pavlov, G.G., & Romani, R.W. 2004, ApJ, 602, 327, arXiv:astro-ph/0310854

Luo, Q., Shibata, S., & Melrose, D.B. 2000, MNRAS, 318, 943

Manchester, R.N., & Johnston, S. 1995, ApJ, 441, L65

Muslimov, A.G., & Harding, A.K. 1997, ApJ, 485, 735 (MH97)

Muslimov, A.G., & Harding, A.K. 2003, ApJ, 588, 430, arXiv:astro-ph/0301023

Muslimov, A.G., & Harding, A.K. 2004, ApJ, in press, arXiv:astro-ph/0408377

Muslimov, A.G., & Tsygan, A.I. 1992, MNRAS, 255, 61 (MT92)

Pavlov, G.G., & Zavlin, V.E. 1997, ApJ, 490, L91, arXiv:astro-ph/9709255

Rudak, B., & Dyks, J. 1999, MNRAS, 303, 477, arXiv:astro-ph/9812212

Usov, V.V. 1983, *Nature*, 305, 409

Van Straten, W., Bailes, M., Britton, M.C., Kulkarni, S.R., Anderson, S.B., Manchester, R.N., & Sarkissian, J. 2001, *Nature*, 412, 158, arXiv:astro-ph/0108254

Venter, C. 2004, M.Sc. Thesis, North-West University, Potchefstroom, Unpublished

Yoshida, T., Yoshikoshi, T., & Yuki, A. 2002, *Astroparticle Physics*, 16, 235

Zavlin, V.E., Pavlov, G.G., Sanwal, D., Manchester, R.N., Trümper, J., Halpern, J.P., & Becker, W. 2002, *ApJ*, 569, 894, arXiv:astro-ph/0112544

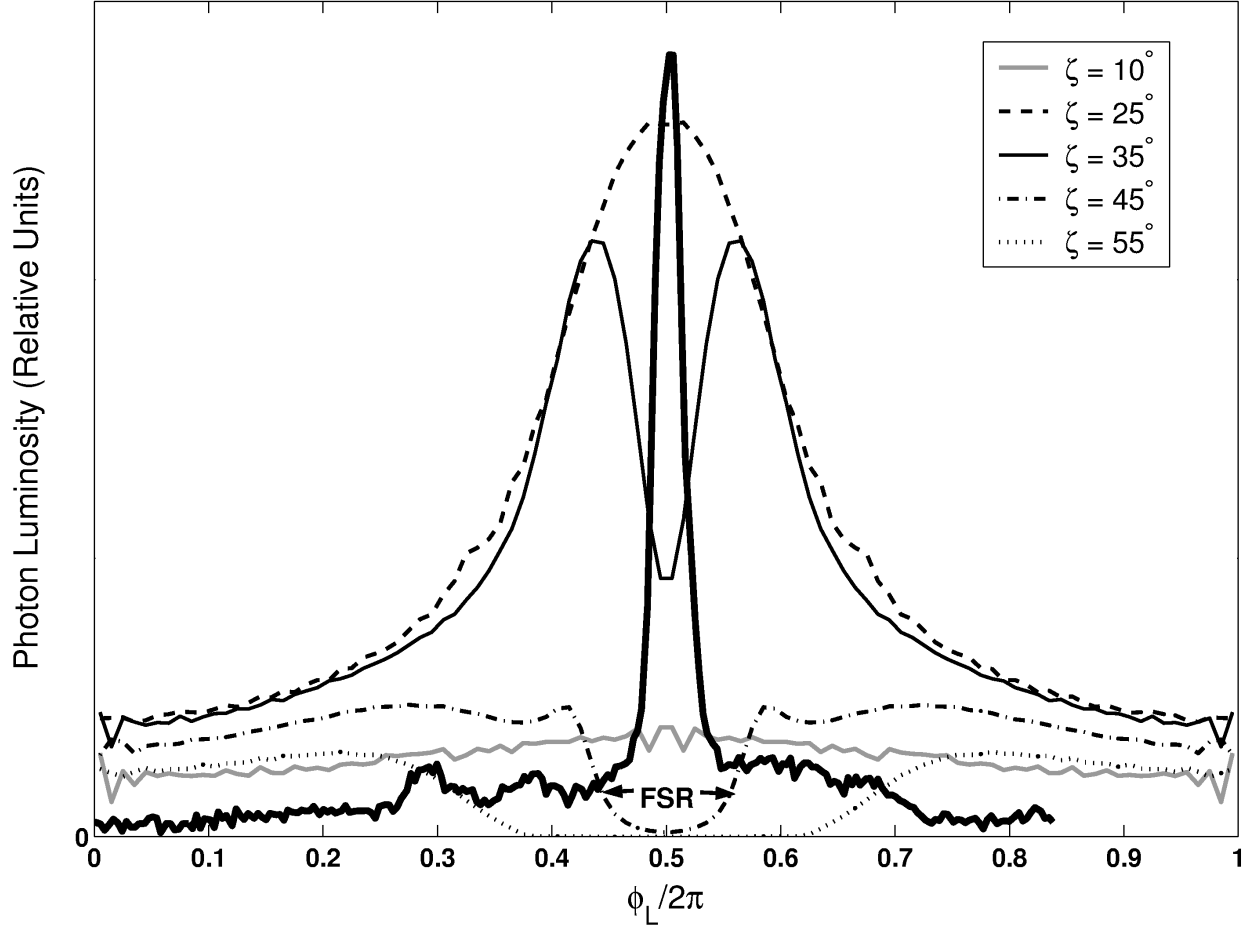


Fig. 1.— Photon luminosity (in relative units) vs. observer pulse phase (with phase 0.5 corresponding either to  $\phi = 0$  or  $\phi = \pi$ , depending on  $\zeta$ ) for PSR J0437-4715 for different  $\zeta$  (see legend). The following parameters were assumed (see text for references):  $P \approx 5.76$  ms (period),  $R_6 = 1.3$ ,  $I_{45} = 1$ ,  $M = 1.58 M_\odot$  and  $\chi = 35^\circ$ . The radio pulse at 4.6 GHz (thick solid line - Manchester & Johnston (1995)) is superimposed for reference (see [www.atnf.csiro.au/research/pulsar/psrcat](http://www.atnf.csiro.au/research/pulsar/psrcat)). The “valleys” at observer phase  $\sim 0.5$  of the lightcurves with  $\zeta \geq \chi$  are probably due to electric field sign reversals (FSR), since the magnetic field lines where these reversals occur, were ignored (see text for details).

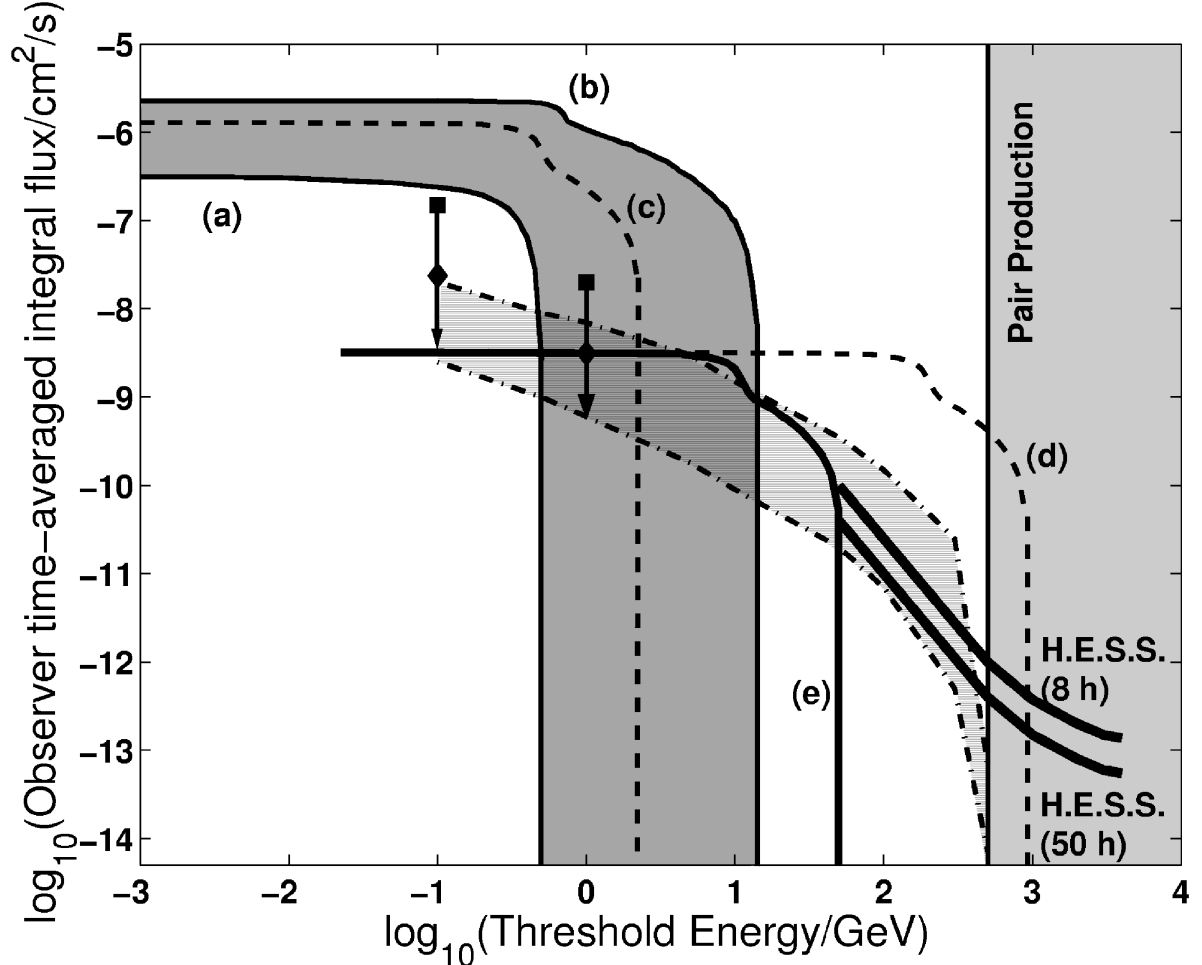


Fig. 2.— Observer time-averaged integral flux vs. threshold energy. Curve (a), for which  $R_6 = 1.7$ ,  $I_{45} = 1$ ,  $\chi = 35^\circ$  and  $\zeta = 40^\circ$  and curve (b) for which  $R_6 = 1.3$ ,  $I_{45} = 3$ ,  $\chi = 20^\circ$  and  $\zeta = 16^\circ$ , define a “confidence band” wherein the integral flux is expected to lie according to the GR model discussed in this paper. Curve (c), for which  $R_6 = 1.5$ ,  $I_{45} = 2$ ,  $\chi = 20^\circ$ , and  $\zeta = 16^\circ$ , represents an intermediate curve. Curve (d) is curve (c) scaled with scale factor  $\lambda = 400$ , while curve (e) is curve (d) shifted to the left (see text for details). The band with dot-dashed curves is that of BRD00 for PSR J0437-4715 for their ‘Model A’. The squares represent EGRET integral flux upper limits (Fierro et al. 1995), while the diamonds represent these upper limits reduced by a factor  $\sqrt{5}$ , appropriate for a beam with main pulse width of  $\sim 0.2$ . Also indicated are the H.E.S.S. sensitivities for 50 hours (Hinton 2004) and 8 hours observation time, and the energy above which pair production is expected to take place (BRD00).